Nonlinear quenches of power-law confining traps in quantum critical systems

Mario Collura[1,2] and Dragi Karevski[1,*]

[1]*Institut Jean Lamour, dpt. P2M, Groupe de Physique Statistique, Nancy-Université CNRS, B.P. 70239,*
F-54506 Vandoeuvre les Nancy Cedex, France
[2]*Institut für Theoretische Physik, Universität Leipzig, Postfach 100 920, D-04009 Leipzig, Germany*

We describe the coherent quantum evolution of a quantum many-body system with a time-dependent power-law confining potential. The amplitude of the inhomogeneous potential is driven in time along a nonlinear ramp which crosses a critical point. Using Kibble-Zurek-like scaling arguments we derive general scaling laws for the density of excitations and energy excess generated during the nonlinear sweep of the confining potential. It is shown that, with respect to the sweeping rate, the densities follow algebraic laws with exponents that depend on the space-time properties of the potential and on the scaling dimensions of the densities. We support our scaling predictions with both analytical and numerical results on the Ising quantum chain with an inhomogeneous transverse field varying in time.

PACS number(s): 03.75.Kk, 03.75.Lm, 05.30.Rt, 32.80.Xx

I. INTRODUCTION

An interesting question about the behavior of a quantum system near a quantum critical point [1] is how the presence of spatially varying external fields, or local modulation of the internal couplings (which may be randomly or deterministically distributed [2]), will influence the equilibrium and dynamical properties of such a system. Depending on the relevance of the perturbation generated by the field or coupling inhomogeneity, the universality class governing the behavior close to the critical point may change [3]. A relevant inhomogeneity may even suppress the very existence of the critical point as, for instance, is trivially the case on a finite-size system [4]. The critical behavior will be modified locally at a boundary, as, for example, at a flat surface, at a corner, or at the tip of a parabolic-shaped system [5]. An extended inhomogeneity may be such that it is too weak to modify the bulk critical behavior but strong enough to change the local critical properties at a surface or at an interface [6]. One may also mention a series of works on gradient percolation, where an inhomogeneous field was introduced as a tool allowing for accurate estimates of the percolation threshold and the percolation exponents [7]. The main effect of such a spatially varying field inhomogeneity is to smooth out the critical singularities. Indeed, the inhomogeneous field leads to a departure from the critical point, which introduces a finite length scale in the problem. More recently, based on the proper identification of the typical length scale, a scaling theory for the equilibrium profiles of energy and particle densities has been developed for quantum systems with power-law inhomogeneities [8–11]. Such power-law fields are particularly relevant in the context of ultracold atoms, where parabolic trapping potentials are used to confine atomic clouds.

Beautiful experiments from the ultracold-gases community have revived the theoretical studies of the nonequilibrium behavior of strongly correlated quantum systems [12]. The main reason for that is that the dynamics of such atomic systems presents a very low dissipation rate and a good phase coherence over very long times [12]. Consequently, the real dynamics are very well modeled by the usual quantum unitary evolution of closed systems. Among the various possible nonequilibrium situations that one may think of, a case that has received much attention is where the parameters of the quantum many-body system are varied in time such that the system reaches or crosses a quantum critical point. In this case, close to the critical point, the divergence of the intrinsic relaxation time leads to a nonadiabatic evolution of the system no matter how slow the Hamiltonian is changed. If the system is initially in its ground state, nonadiabatic transitions toward excited states lead to the generation of topological defects in the final state [13–17]. For example, driving a quantum system from a paramagnetic to a ferromagnetic phase through a critical point generates a final state given by a superposition over excited states carrying finite ferromagnetic domains separated by kinks or domain walls. For a slow driving rate, the density of defects is a universal scaling function of the driving rate, as in the classical Kibble-Zurek (KZ) mechanism [18]. This may be of importance in the context of adiabatic quantum computation [19], where adiabatic evolution is proposed to transfer the system from an initial state to a computational nontrivial state. If one is forced to cross a critical point in order to generate the nontrivial state, inevitably the crossing will result in the generation of excitations (defects). The optimal time ramp needed to drive the system through the critical point has to balance the unavoidable generation of defects and the time needed to cross the critical point [17].

Removing or loading a power-law trap smoothly in time and close to a critical point, as sketched in Fig. 1, will lead to a final state carrying a nontrivial density of defects, which will depend on the shape of the trap, as we have shown in a recent letter [20]. The reason for this result is the fact that the power-law perturbation is a relevant one and modifies the universality class of the critical point, leading to an effective correlation length exponent which has to enter into the Kibble-Zurek prediction instead of the original one. In this article, we analyze in detail the coherent generation of defects during such an inhomogeneous quench [20]. A general scaling argument is presented from which the scaling behavior of local (such as the local energy density or order parameter) and global
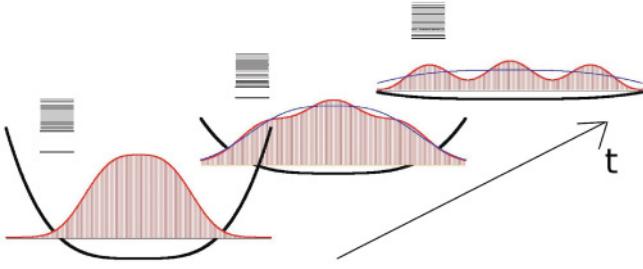
———————
[*]karevski@lpm.u-nancy.fr

FIG. 1. (Color online) Sketch of the problem we consider in this article.

(such as the density of defects) quantities are derived. The minimization of defect production for a given total sweeping time is also discussed within the scaling approach. Aside from the scaling-argument approach, we also present an analytical near-adiabatic analysis and an exact numerical study of the Ising quantum chain with an inhomogeneous transverse field playing the role of the confining potential.

The article is organized in the following way: The next section is devoted to the scaling theory. The dynamical analysis is presented in Sec. III and the specific case of the Ising model is treated in Sec. IV. Finally, we summarize our results in Sec. V.

II. SCALING THEORY

A. Scaling arguments

The d-dimensional quantum system we consider has a quantum critical point at zero temperature governed by a scalar field h. The critical point separates a symmetric phase from a broken-symmetry phase. The homogenous critical field value is h_c. We assume that, close enough to the critical point, the quantum control parameter h deviates in one direction from the homogeneous critical value h_c with a power law

$$\delta(x,t) \equiv h(x,t) - h_c \simeq g(t)|x|^{\omega}, \quad (1)$$

with a positive space exponent $\omega > 0$. The amplitude $g(t)$ of the spatial deviation of the critical value [which is set fixed at $x = 0 \,\forall\, t$ according to (1)] is driven externally from a given initial value to a final value following the nonlinear time ramp

$$g(t) = v|t|^{\alpha}\text{sgn}(t), \quad (2)$$

with α a positive exponent, $\text{sgn}(t)$ the sign function, and where, without loss of generality, the rate amplitude v is assumed to be positive and determines the velocity of the quench. For small v, the quench is slow, whereas it is faster at larger values. Notice that, within the following parametrization, the quench dynamics connect the two distinct phases by crossing the homogeneous critical point [$h(x) = h_c \,\forall\, x$] at time $t = 0$. Negative times correspond to the $\delta < 0$ phase while positive times correspond to the $\delta > 0$ phase.

The presence of the inhomogeneous field (1) introduces a crossover region in space-time (x,t) around the critical locus $(0,0)$ with characteristic length scale ℓ and time scale τ. To see that, let us start in the far past, at $t = -T$ with $T \gg 1$, from the ground state $|\text{GS}(g(-T))\rangle$ associated with the initial amplitude $g(-T)$. Under the unitary dynamics generated by the time-dependent Hamiltonian, the system

starts to evolve adiabatically, following the instantaneous ground state $|\text{GS}(g(t))\rangle$ as far as it is protected from transitions to excited states by a large energy gap $\Delta(t)$ between the ground state and excited states. At time t, in the instantaneous state $|\text{GS}(g(t))\rangle$, the spatial power-law deviation of the control parameter δ from the critical point introduces a finite length scale $\ell(t)$ around the spatial critical locus (here at $x = 0$) [8]. The typical length can be obtained self-consistently by noting that, with this width, $\ell(t)$ is associated with a given deviation $\delta(\ell) = g\ell^{\omega}$ from which a characteristic length $\delta(\ell,t)^{-\nu}$ can be constructed from the correlation length relationship. From the identification $\ell(t) \sim \delta(\ell,t)^{-\nu}$ one finally finds

$$\ell(t) \sim |g(t)|^{-\nu/(1+\nu\omega)}. \quad (3)$$

The typical length scale $\ell(t)$ diverges for a vanishing deviation amplitude g that is close to the critical point with an effective correlation length exponent given by

$$\nu_g \equiv \frac{1}{y_g} = \frac{\nu}{1+\nu\omega}. \quad (4)$$

As time runs toward zero, the energy gap Δ of the system vanishes and, correspondingly, the relaxation time $\propto 1/\Delta$ gets larger and larger up to the point where the adiabatic evolution breaks down completely due to the contributions of the transitions toward instantaneous excited states. When sufficiently close to the homogeneous critical point, the response of the system to the external driving is so slow that the dynamics switch to a sudden regime. After the critical point has been crossed, for sufficiently large times, one recovers again the nearly adiabatic regime. The typical time scale τ around the critical locus, separating the nearly adiabatic dynamics from the sudden-quench regime, can be deduced from the self-consistent relation $\tau \sim \ell(\tau)^z$, where z is the dynamical exponent. This leads to

$$\tau \sim \ell^z \sim v^{-z/y_v}, \quad (5)$$

where

$$\frac{1}{\nu_v} \equiv y_v = y_g + z\alpha = \frac{1+\nu(\omega+z\alpha)}{\nu}, \quad (6)$$

is the Renormalization Group (RG) dimension of the perturbation field, such that, under rescaling by a factor b, the amplitude v transforms as $v' = b^{y_v}v$. Since ω and α are positive, the perturbation is always relevant ($y_v > 0$). Notice that, within the quench, the maximal extension of the length scale ℓ scales with the rate amplitude v as $\ell \sim v^{-\nu_v}$, where ν_v plays the role of an effective correlation length exponent for the effective thermal field v. For a given value of v, the typical length scale never diverges, even exactly when we cross the critical point since, before that, there is a critical slowing down which freezes completely the dynamics and avoids then the further development of correlations.

The scaling of the profile of a local quantity $\phi(x,t,v)$, like the local order parameter or the energy density with scaling dimension x_{ϕ} close to the critical locus, is determined under the homogeneity hypothesis $\phi(x,t,v) = b^{-x_{\phi}}\phi(xb^{-1},tb^{-z},vb^{y_v})$. Taking the rescaling factor to be $b = v^{-1/y_v} \propto \ell \propto \tau^{1/z}$, one obtains

$$\phi(x,t,v) = v^{x_{\phi}/y_v}\Phi(xv^{1/y_v},tv^{z/y_v}), \quad (7)$$

where Φ is a scaling function. As discussed previously, the prefactor exhibits the trap-size scaling $\phi \sim \ell^{-x_\phi}$ associated to the finite-size scale $\ell \sim v^{-1/y_v}$ [8]. Notice here that the scaling form (7) is not expected to be valid outside the critical region, that is for $|x| \gg \ell$ since, in those regions, the field values are very far from the critical value.

In the same way, if we are interested only in the time evolution of the spatial-averaged quantity, after integration in space over the critical domain ℓ of the preceding equation, one obtains

$$\overline{\phi}(t,v) = \frac{1}{\ell} \int_\ell dx\, \phi(x,t,v)$$
$$= v^{x_\phi/y_v}\overline{\Phi}(tv^{z/y_v}) \sim \tau^{-x_\phi/z}\overline{\Phi}\left(\frac{t}{\tau}\right). \quad (8)$$

As an example, the averaged energy density should behave after the quench to the critical point as $e \sim v^{(d+z)/y_v}$ since its scaling dimension is $x_e = d + z$ [21].

B. Density of defects

The defect production generated during the quench by crossing the critical point is deduced through the identification of the typical Kibble-Zurek time scale corresponding to the freezing of the dynamics. Equating the relaxation time $\kappa/\Delta(t)$ with the typical time-scale $\Delta(t)/|\dot{\Delta}(t)|$ at which the Hamiltonian is varied and assuming that the gap scales as $\Delta(t) \simeq \Omega_0 |g(t)|^{z/y_g}$, one finds for the typical (Kibble-Zurek) time scale

$$\tau_{\mathrm{KZ}} \sim \left(\frac{\kappa}{\Omega_0}\frac{z\alpha}{y_g}\right)^{y_g/y_v} v^{-z/y_v}. \quad (9)$$

The defect density being proportional to the inverse of the correlation volume at the Kibble-Zurek time, one obtains from the relationship $n \sim [\Delta(\tau_{\mathrm{KZ}})]^{d/z}$ the behavior

$$n \sim \left(\frac{\kappa}{\Omega_0}\frac{z\alpha}{y_g}\right)^{d\alpha/y_v} v^{d/y_v} = (z\gamma\delta)^{\frac{d\gamma}{1+z\gamma}}, \quad (10)$$

with $\delta = \frac{\kappa}{\Omega_0}v^{1/\alpha} \sim 1/T$ (with T defining the temporal window of the quench protocol) and $\gamma = \alpha v_g = \alpha/y_g$. As one would expect, the density of defects n is smaller for larger values of the protocol time window T used to reach a final value g_{f} from the initial g_0 value. The obvious conclusion is that, if one wants to minimize the generation of defects, the switching of the trap should be as slow as possible. However, this can lead to extremely long protocol times T and be counterproductive as, for example, in quantum computational issues where one looks for a compromise between the production of excited states and short computational times. In order to achieve this compromise, one may look for the optimal power-law time-ramp protocol that minimizes the defect density n at a fixed duration T. Optimizing (10) with respect to $\gamma = \alpha/y_g$ for a given $\delta \sim 1/T$ one finds

$$\gamma_{\mathrm{opt}} = \frac{1}{z}W\left(\frac{1}{e\delta}\right), \quad (11)$$

where $\mathcal{W}(x)$ is the Lambert $\mathcal{W}$ function defined through $x = f(\mathcal{W}) = \mathcal{W}e^{\mathcal{W}}$. For a given trap shape (space exponent ω fixed) the optimum time exponent takes the value $\alpha_{\mathrm{opt}} =$

$\gamma_{\mathrm{opt}}/v_g = \gamma_{\mathrm{opt}}(1 + v\omega)/v$. Using the asymptotic expansion of the Lambert function $\mathcal{W}(x) \simeq \ln x - \ln(\ln x)$ at large x, the result of [17] is recovered with $\omega = 0$:

$$\alpha_{\mathrm{opt}} \simeq -\frac{1}{zv}\ln\left(e\delta\ln\frac{1}{e\delta}\right). \quad (12)$$

Loading a power-law trap potential changes significantly the value of the optimal temporal exponent α, increasing it by a factor $(1 + v\omega)$. This means that, with a power-law trap and close to the critical point, one has to drive the system slower than without a trap in order to minimize the defect production.

In view of the scaling prediction (7) we expect the density of defects $n(x,v)$ produced locally within the critical region to scale as

$$n(x,v) = v^{d/y_v}\mathcal{N}(xv^{1/y_v}) = \ell^{-d}\mathcal{N}\left(\frac{x}{\ell}\right), \quad (13)$$

where we have set $t = \tau_{\mathrm{KZ}} = v^{-z/y_v}$. The unknown scaling function $\mathcal{N}(u)$ should go to a constant as $u \to 0$.

C. Global shift to the critical point

A question that may naturally arise is about the validity of the present approach when the critical locus is not exactly at the expected space-time location, as would certainly be the case in an experiment. If there is an uncertainty in the locus of the critical point, following [22], we can distinguish several situations. First of all, if the deviation to the expected locus is due to a shift δ_g in the time ramp amplitude such that the actual perturbation is given by

$$\delta(x,t) \simeq [g(t) - \delta_g]|x|^\omega, \quad (14)$$

where, without loss of generality, we assume $\delta_g > 0$, then the critical point is crossed [for $g(t^*) = \delta_g$] at $t^* = (\delta_g/v)^{1/\alpha}$. Developing $\delta(x,t)$ near t^* (and neglecting higher-order contributions) we obtain

$$\delta(x,t) \simeq \left.\frac{\partial\delta(x,t)}{\partial t}\right|_{t^*}(t - t^*) = \hat{v}_g(t - t^*)|x|^\omega, \quad (15)$$

where we have identified a new rate $\hat{v}_g = \alpha v^{1/\alpha}\delta_g^{1-1/\alpha}$. The effect of a finite δ_g leads then to an effective linear time ramp without changing the spatial behavior. Our scaling predictions hold then with the time exponent α replaced by the new time exponent $\hat{\alpha} = 1$ and the rate v by the effective rate $\hat{v}_g$.

If the deviation to the critical point is due to a global residual shift δ_h such that the actual trap has the form $\delta(x,t) = g(t)|x|^\omega - \delta_h$, one has to distinguish between a small shift and a relatively large one. Consider first the case of a small global shift δ_h, such that we are still in a scaling regime. The scaling dimension associated to the global shift is that of the unperturbed system $1/v$. Under rescaling by a factor b, the length scale and time scale change according to

$$b^{-1}\ell(v,\delta_h) = \ell(vb^{y_v},\delta_h b^{1/v}), \quad b^{-z}\tau = \tau(vb^{y_v},\delta_h b^{1/v}), \quad (16)$$

which leads to taking vb^{y_v} to

$$\ell = v^{-1/y_v}\tilde{\ell}(\delta_h v^{-1/vy_v}), \quad \tau = v^{-z/y_v}\tilde{\tau}(\delta_h v^{-1/vy_v}). \quad (17)$$

The scaling functions $\tilde{\ell}(u)$ and $\tilde{\tau}(u)$ have to satisfy the limiting behavior $\tilde{\ell}(0) = \ell_0$, $\tilde{\tau}(0) = \tau_0$ and, for $u \gg 1$,

$$\tilde{\ell}(u) \sim u^{-\nu}, \quad \tilde{\tau}(u) \sim u^{-z\nu},$$

in order to match the usual scaling in absence of the trap. Physically, these assumptions mean that the shortest length between $\xi_h \sim \delta_h^{-\nu}$ and $\ell_v \sim v^{-1/y_v}$ dominates the behavior near the critical locus. The trap-size scaling (7) is expected to hold when $1 \ll \ell_v \ll \xi_h$; that is, when the system is critical enough in the absence of the trapping potential. The general scaling for a local field is given by

$$\phi(x,t,v,\delta_h) = b^{-x_\phi} \Phi(xb^{-1}, tb^{-z}, vb^{y_v}, \delta_h b^{1/\nu}), \quad (18)$$

and again with $vb^{y_v} = 1$ we have the following trap-size scaling

$$\phi(x,t,v,\delta_h) = v^{x_\phi/y_v} \Phi(xv^{1/y_v}, tv^{z/y_v}, \delta_h v^{-1/\nu y_v}), \quad (19)$$

which is nothing but the scaling

$$\phi(x,t,v,\delta_h) = \ell_v^{-x_\phi} \tilde{\Phi}\left(\frac{x}{\ell_v}, \frac{t}{\ell_v^z}, \frac{\xi_h}{\ell_v}\right). \quad (20)$$

Under this new scaling assumption we have, in particular, an energy gap of

$$\Delta(v,\delta_h) \simeq v^{z/y_v} \Omega(\delta_h v^{-1/\nu y_v}). \quad (21)$$

For $\delta_h \ll 1$ and $v \to 0$ we have to recover the homogeneous behavior $\Delta \sim \delta_h^{z\nu}$, which imposes $\Omega(u) \sim u^{z\nu}$ for $u \gg 1$. For $\delta_h v^{-1/\nu y_v} \to 0$ developing the function Ω close to zero we obtain

$$\Delta(v) \simeq \Omega_0 v^{z/y_v} + \Omega_0' v^{(z\nu-1)/\nu y_v} \delta_h + o(\delta_h). \quad (22)$$

For the defect density, from the Kibble-Zurek prediction $n \sim \Delta^{d/z}$ one obtains the behavior

$$n \sim \Omega_0 v^{d/y_v} \left(1 + \frac{\Omega_0'}{\Omega_0} v^{-1/\nu y_v} \delta_h + o(\delta_h)\right)^{d/z}$$

$$\simeq \Omega_0 v^{d/y_v} + \frac{d}{z} \Omega_0' v^{d/y_v - 1/\nu y_v} \delta_h + o(\delta_h). \quad (23)$$

For the special case of the Ising quantum chain that we consider in the following, we have $d = 1$, $\nu = 1$, and $z = 1$, then, to the first order in δ_h, the corrections are independent of v:

$$n_{\text{Ising}} \sim \Omega_0 v^{1/(1+\omega+\alpha)} + \Omega_0' \delta_h + o(\delta_h), \quad (24)$$

generating a constant shift to the original behavior.

For a large constant shift δ_h taking the system out of the previous scaling regime, we have to distinguish between negative and positive global shifts. In order to fix the ideas for the discussion, let us set $g(t) = -v|t|^\alpha \text{sgn}(t)$ and drive the system from an initial negative time $t_i = -t_0$ to $t = 0$ where the coupling profile is completely flat: $\delta(x,0) = -\delta_h$. If δ_h is negative then, since $\delta(x,t) \geqslant |\delta_h| \; \forall \; x$, the system stays in its disordered phase during the full evolution. Its dynamics are always nearly adiabatic since, at any time $t \in [-t_0, 0]$, the gap remains large enough for $|\delta_h| = O(1)$. One expects in this case an exponentially small defect generation. On the contrary, for a positive global shift δ_h there is at each time a region around $x = 0$ which is already in the symmetry-broken phase [negative $\delta(x,t)$ values]. During the time evolution from

$t = -t_0$ to $t = 0$, this area around the origin $x = 0$ will grow, propagating the symmetry-broken phase into the symmetric phase [22]. The temporal dependence of the critical front $x^*(t)$, separating both phases, determined from the critical locus condition $\delta(x^*,t) = 0$ is given by

$$|x^*(t)| = \left(\frac{\delta_h}{v}\right)^{1/\omega} (-t)^{-\alpha/\omega} \quad \text{with} \quad t \in [-t_0, 0]. \quad (25)$$

Since α and ω are both positive, the critical locus $x^*(t)$ is expelled to infinity as we approach $t = 0$. At the beginning of the quench, the critical locus front propagates slowly enough that the ordered phase extends into the disordered phase with a very low rate of defect generation. However, as time approaches zero, the velocity of the front becomes very large such that there is no longer a causal connection with the already nucleated ordered phase and the disordered phase. This leads to an effective sudden quench regime for the part of the system which is outside the causal region. In order to obtain the dependence of the threshold point x_0 after which the causality is lost, we develop $\delta(x,t)$ near, lets say, the positive critical front $x^*(t) > 0$. Close to x^*, one has a linear front

$$\delta(x,t) \simeq \left. \frac{\partial \delta(x,t)}{\partial x} \right|_{x^*(t)} [x - x^*(t)] = \hat{v}_h(-t)^{\alpha/\omega}[x - x^*(t)],$$

$$(26)$$

with a local slope $\hat{v}_h(-t)^{\alpha/\omega}$, where the rate $\hat{v}_h = \omega v^{1/\omega} \delta_h^{1-1/\omega}$. Notice here that the slope of the linear front is decaying as $t \to 0$ as $|t|^{\alpha/\omega}$; that is, as the trap is opening. This front drives locally the system from one phase to the other with a time-dependent velocity $c^*(t) \equiv dx^*/dt \sim x^{*1+\omega/\alpha}(v/\delta_h)^{1/\alpha} \sim x^*(t)/t$. As was pointed out in [22], the propagation of the front turns out to suppress the Kibble-Zurek excitations in a region around the origin and rejects the defect production outside this region. At the critical locus x^*, the linearized perturbation introduces a local length scale $\ell^*(t) = \ell(x^*(t)) \sim [\delta_h/x^*(t)]^{-\nu/(1+\nu)}$ and time scale $\tau^*(t) \sim \ell^*(t)^z$ according to the scaling argument (3) developed in the introduction (see [8]). To get an idea of the extension of that region, we compare the velocity $c^*(t)$ of the front with the typical velocity, close to x^*, $\ell^*(t)/\tau^*(t) \sim \ell^*(t)^{1-z}$. From that, one may extract a time τ_0, where both velocities become of the same order, and then deduce the threshold locus $x_0 \equiv x^*(\tau_0)$. In the case of the Ising chain treated below, since the critical exponents $z = \nu = 1$, the system enters into the sudden regime as soon as the front velocity $c^*(t)$ is larger than the sound velocity (hereafter set to one). One obtains from the equation $c^*(\tau_0) = 1$

$$x_0 = x^*(\tau_0) \sim \tau_0 \sim \left(\frac{\delta_h}{v}\right)^{1/(\alpha+\omega)}. \quad (27)$$

Around the point x_0 one expects a critical region with typical fluctuations of order $(x_0/\delta_h)^{\nu/(1+\nu)} = \sqrt{x_0/\delta_h}$ since, for the Ising chain, $\nu = 1$.

III. DYNAMICAL ANALYSIS

A. Adiabatic approximation

If the time-variation of the Hamiltonian is slow enough, one can use a nearly adiabatic approximation in order to describe the actual state $|\Psi(t)\rangle = \mathcal{U}(t,t_0)|0(t_0)\rangle$ obtained from the initial

ground state $|GS\rangle = |0(t_0)\rangle$ of the initial Hamiltonian $\mathcal{H}(t_0)$. Introducing the instantaneous eigenbasis $\{|k(t)\rangle\}$ (which is assumed to be discreet for simplicity) $\mathcal{H}(t)|k(t)\rangle = E_k(t)|k(t)\rangle$ one obtains from standard perturbation theory the "one-jump" expansion

$$|\Psi(t)\rangle \approx e^{-i\int_{t_0}^{t} ds\, E_0(s)} \Bigg[|0(t)\rangle$$
$$+ \sum_{k\neq0} |k(t)\rangle \int_{t_0}^{t} dt' \langle \dot{k}(t')|0(t')\rangle e^{-i\vartheta_k(t',t)} \Bigg], \quad (28)$$

where $\vartheta_k(t',t) = \int_{t'}^{t} ds\, \delta\omega_{k0}(s)$ with the Bohr frequency $\delta\omega_{k0}(t) \equiv E_k(t) - E_0(t)$. Notice that this expansion is valid only if the eigenvectors are changing continuously with time. The first term on the right-hand side is the usual adiabatic result: the state is in the instantaneous eigenstate $|0(t)\rangle$ (here the ground state) of the Hamiltonian $\mathcal{H}(t)$ multiplied by a dynamical phase factor. It corresponds to no jump at all. The second term is the "one-jump" contribution. It represents an adiabatic evolution from the initial state up to a time t', a sudden transition at t' toward an excited state $|k(t')\rangle$, followed by an adiabatic evolution from $|k(t')\rangle$ to $|k(t)\rangle$. The total contribution results from the integration over all times $t' \in [t_0,t]$ at which the transition could take place, and then summed over all transition states. Higher-order terms are built by taking into account more than one single jump between the instantaneous states and are neglected here. Using the identity $\langle \dot{k}(t)|q(t)\rangle = \langle k(t)|\partial_t\mathcal{H}(t)|q(t)\rangle/\delta\omega_{kq}$ for $k \neq q$, the transition amplitudes $a_k(t_0,t) = \langle k(t)|\Psi(t)\rangle$ (up to a global phase factor) are given by

$$a_k(t_0,t) = \int_{g(t_0)}^{g(t)} dg\, \frac{\langle k(g)|\partial_g\mathcal{H}(g)|0(g)\rangle}{\delta\omega_{k0}(g)} e^{-i\vartheta_k(g,g(t))}, \quad (29)$$

where the phase factor is given by

$$\vartheta_k(x,y) = \frac{v^{-1/\alpha}}{\alpha} \int_x^y dg\, |g|^{1/\alpha-1}\delta\omega_{k0}(g). \quad (30)$$

The density of defects generated with the nonlinear ramp $g(t)$ is given by summing the transition probabilities $|a_k|^2$ over all the excited states $|k(g)\rangle$. To analyze the behavior of the transition amplitude we need to know the behavior of the energy spectrum $\delta\omega_{k0}(g)$ and of the perturbation matrix elements $\langle k(t)|\partial_t\mathcal{H}(t)|q(t)\rangle$, which will depend on the precise space- and time-dependence of the perturbation field. The scaling of $\delta\omega_{k0}$ is linked to the scaling of the energy density $e(x,\ell) = \ell^{-(d+z)}\mathcal{E}(x/\ell)$, according to the trap-size scaling developed in the preceding section by a space integration. This leads to $\delta\omega_{k0} \sim \ell^{-z}\Omega(\ell^{-z}/k^z)$. Along the same lines, dimensionally one expects $\langle k(g)|\partial_g\mathcal{H}(g)|0(g)\rangle \sim \ell^{-z}G(\ell^{-z}/k^z)/g \sim \ell^{-z+y_g}G(\ell^{-z}/k^z)$, where $\ell \sim g^{-1/y_g}$ is the typical length introduced by the spatial perturbation at time t. For the integral (29) to converge at $g = 0$ (i.e., for a quench crossing the critical point), the scaling function $F(u) = G(u)/\Omega(u)$ has to decay to zero at least linearly at small u, which is the case for the spatially homogeneous quench [1,16]. Plugging these assumptions into (29), the excitation density generated by crossing the critical point was found to scale as $n \simeq C v^{\frac{dv}{1+vz\alpha}}$, which is nothing but $n \sim \ell^{-d}$ with $\ell \sim v^{-\frac{v}{1+vz\alpha}}$ for $\omega = 0$ [16]. In the spatially inhomogeneous situation the convergence close to the critical point is not

guaranteed (see below the analytical example of the Ising chain with $\omega = 1$). Consequently, one cannot in general use the first-order perturbation expansion (29) for a quench crossing the critical point. Nevertheless, the adiabatic approximation can be used for quenches that take the system close to the critical point without crossing it. Getting closer and closer to the critical point, the transition amplitudes will display a scaling signature.

IV. ISING QUANTUM CHAIN

A. Diagonalization and nearly adiabatic dynamics

Let us consider the specific case of the Ising quantum Hamiltonian in a time-dependent inhomogeneous transverse field:

$$\mathcal{H}(t) = -\frac{1}{2}\sum_{n=1}^{L-1}\sigma_n^x\sigma_{n+1}^x - \frac{1}{2}\sum_{n=1}^{L}h_n(g)\sigma_n^z, \quad (31)$$

where $h_n(g) = 1 + g(t)n^\omega$, with $g(t) = v|t|^\alpha \text{sgn}(t)$. Because it is integrable, this model has been used extensively as a standard theoretical laboratory for issues related to quantum phase transitions [1]. Let us recall that, in the unperturbed case ($h_n = h\ \forall\ n$), the system presents a critical point at $h = 1$ separating a disordered phase (for $h > 1$) from a symmetry-broken ordered phase at $h < 1$. The dynamical exponent $z = 1$ and the (thermal) correlation length exponent $\nu = 1$. More recently, it became a favorite test model in various out-of-equilibrium situations such as those generated by suddenly quenching its transverse field from a given initial value to a new value [23]. In this study, the inhomogeneous time-dependent field plays a role similar to a trapping potential. The spatial critical locus has been set at the left boundary of the chain (one could have also considered the case of a centered critical locus without real differences from what follows).

In order to diagonalize (31), one may perform a Jordan-Wigner transformation mapping the Pauli matrices into fermionic operators. In term of Clifford's operators (Majorana fermions)

$$\Gamma_n^1 = \prod_{j=1}^{n-1}\left(-\sigma_j^z\right)\sigma_n^x, \quad \Gamma_n^2 = -\prod_{j=1}^{n-1}\left(-\sigma_j^z\right)\sigma_n^y, \quad (32)$$

with $\Gamma_n^{i\dagger} = \Gamma_n^i$ satisfying the anticommutation rules $\{\Gamma_n^i, \Gamma_m^j\} = 2\delta_{ij}\delta_{nm}$, the Hamiltonian (31) takes the quadratic form

$$\mathcal{H}(t) = \tfrac{1}{4}\boldsymbol{\Gamma}^\dagger\mathbf{T}(g)\boldsymbol{\Gamma}, \quad (33)$$

where $\boldsymbol{\Gamma}^\dagger = (\boldsymbol{\Gamma}^{1\dagger}, \boldsymbol{\Gamma}^{2\dagger})$ is the $2L$-component row vector with $\boldsymbol{\Gamma}^{i\dagger} = (\Gamma_1^{i\dagger}, \ldots, \Gamma_L^{i\dagger})$ for $i = 1,2$. The $2L \times 2L$ hermitian matrix $\mathbf{T}(g)$ is given by

$$\mathbf{T}(g) = \begin{pmatrix} \emptyset & \mathbf{C}(g) \\ \mathbf{C}^\dagger(g) & \emptyset \end{pmatrix}, \quad (34)$$

where $\mathbf{C}(g)$ is the interaction matrix with elements

$$C_{mn}(g) = -i[h_n(g)\delta_{mn} + \delta_{mn+1}]. \quad (35)$$

Introducing at each value of g (i.e., at each time), the (instantaneous) eigenvectors

$$V_p(g) = \frac{1}{\sqrt{2}}\begin{pmatrix} \phi_p(g) \\ -i\psi_p(g) \end{pmatrix} \quad (36)$$

of the eigenvalue problem $\mathbf{T}(g)V_p(g) = \epsilon_p(g)V_p(g)$, one can map the Clifford operators onto a set of diagonal Fermi operators:

$$\eta_p(g) = \frac{1}{2}\sum_{n=1}^{L}\left\{\phi_p(n,g)\Gamma_n^1 + i\psi_p(n,g)\Gamma_n^2\right\},$$
$$\eta_p^\dagger(g) = \frac{1}{2}\sum_{n=1}^{L}\left\{\phi_p(n,g)\Gamma_n^1 - i\psi_p(n,g)\Gamma_n^2\right\}, \tag{37}$$

where the fermionic creation and annihilation operators $\eta_p^\dagger(g)$ and $\eta_p(g)$ satisfy the canonical Fermi-Dirac anticommutation rules $\{\eta_p^\dagger(g),\eta_q(g)\} = \delta_{pq}$ for the same value of g. In terms of this new set of operators, the Hamiltonian takes the diagonal form

$$\mathcal{H}(t) = \sum_{p=1}^{L}\epsilon_p(g)[\eta_p^\dagger(g)\eta_p(g) - 1/2], \tag{38}$$

where $\epsilon_p(g)$ are the positive eigenvalues of $\mathbf{T}(g)$. Consequently, the instantaneous ground state $|GS(g(t))\rangle$ is the instantaneous vacuum state $|0(g)\rangle$ destroyed by all the $\eta(g)$'s: $\eta_q(g)|0(g)\rangle = 0 \ \forall q$.

As shown in [11], in the scaling limit $g \to 0$, $L \to \infty$ while keeping gL^ω constant [24], under the rescaling

$$x = |g|^{-1/y_g}u, \quad \epsilon_k = |g|^{1/y_g}\Omega_k,$$
$$\phi_k = |g|^{1/2y_g}\tilde{\phi}_k, \quad \psi_k = |g|^{1/2y_g}\tilde{\psi}_k, \tag{39}$$

with $1/y_g = 1/(1+\omega)$, one obtains from the eigenvalue problem the following differential equations:

$$\left[\frac{d^2}{du^2} + \Omega_k^2 - \text{sgn}(g)\omega u^{\omega-1} - u^{2\omega}\right]\tilde{\phi}_k(u) = 0,$$
$$\left[\frac{d^2}{du^2} + \Omega_k^2 + \text{sgn}(g)\omega u^{\omega-1} - u^{2\omega}\right]\tilde{\psi}_k(u) = 0, \tag{40}$$

with boundary conditions $\partial_u\tilde{\phi}|_0 = 0$, $\tilde{\phi}(\infty) = 0$ and $\tilde{\psi}(0) = 0$, $\partial_u\tilde{\psi}|_\infty = 0$. When g changes sign the two equations are exchanged but the boundary conditions remain the same. The scaling relation (39) with the normalization condition of the solution $(\tilde{\phi}_k, \tilde{\psi}_k)$ assures the correct normalization of the eigenvectors (ϕ_k, ψ_k).

In terms of the diagonal Fermi operators, the perturbation $\partial_g\mathcal{H}(g)$ takes the form

$$\partial_g\mathcal{H}(g) = \frac{1}{2}\sum_{p,q}X_{pq}^\omega(g)[\eta_p^\dagger(g) + \eta_p(g)][\eta_q^\dagger(g) - \eta_q(g)], \tag{41}$$

with $X_{pq}^\omega(g) = \sum_n \phi_p(n,g)n^\omega\psi_q(n,g)$ expressed in terms of the Bogoliubov coefficients ϕ and ψ. Consequently, the time-dependent part of the Ising Hamiltonian induces transitions from the ground state to the two-particle states $|pq(g)\rangle = \eta_q^\dagger(g)\eta_p^\dagger(g)|0(g)\rangle$ only. The nonvanishing perturbation matrix elements are given by

$$\langle pq(g)|\partial_g\mathcal{H}(g)|0(g)\rangle = \frac{1}{2}\Delta_{pq}(g), \tag{42}$$

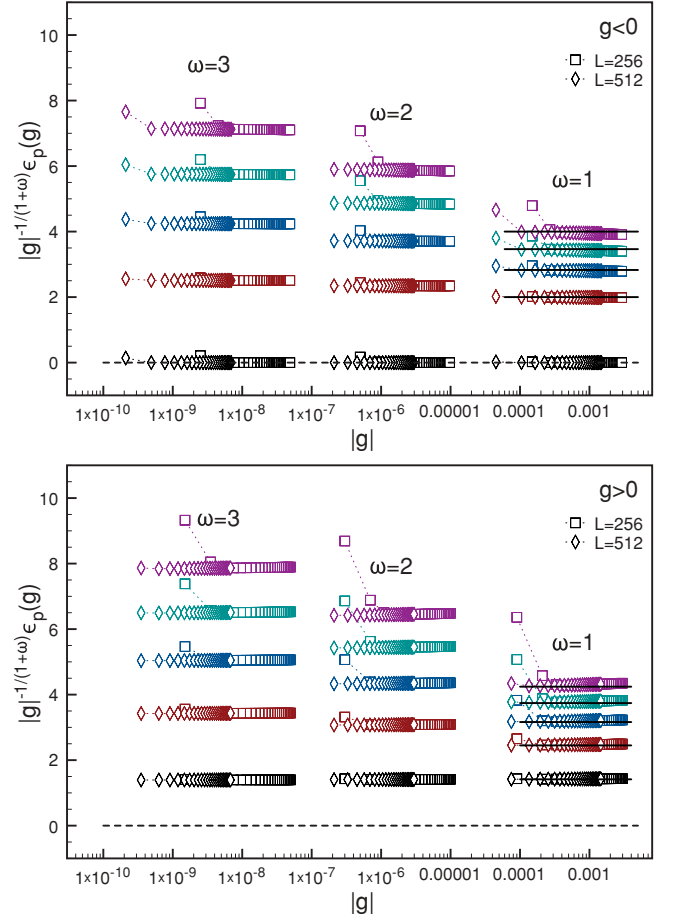FIG. 2. (Color online) The first five Ising one-particle energy levels for different values of the exponent ω in the ordered phase ($g < 0$) and in the disordered phase ($g > 0$). The value of the gradient g varies in order to keep gL^ω sufficiently small [we have used $L = 256$ (squares) and $L = 512$ (diamonds) for the numerical diagonalization] and to fulfill the scaling hypothesis $gL^\omega \ll 1$. The plateau region shows the range of validity of the scaling relation $\epsilon_k = |g|^{1/(1+\omega)}\Omega_k$ in the sense that, in the scaling limit $g \to 0$, $L \to \infty$, all the dependence on the gradient g is encoded in the power-law factor $|g|^{1/(1+\omega)}$. In other words, in the range of validity of the scaling hypothesis, $\partial_g\Omega_k = 0$. Otherwise, for different shapes of the spatial potential (different ω) we have, in the scaling limit, different differential equations and thus different eigenvalues and eigenvectors. Summarizing, the dispersion law $\Omega_k(\omega)$ depends on ω. This is the reason why the plateaus are shifted for different values of ω. In particular, for $\omega = 1$, the straight lines show the analytical dispersion law in Eq. (51). The deviation for small values of the gradient is a finite-size effect which is getting smaller and smaller as the system size is increased. The dashed line indicates the zero energy, showing the existence of a vanishing excitation in the ordered phase.

with $\Delta_{pq}(g) = F_{qp}(g) - F_{pq}(g)$. In the continuum limit, using the scaling variables (39), we can write $F_{pq}(g)$ as an integral over the u variable:

$$F_{pq}(g) = |g|^{-\omega/(1+\omega)}\int_0^\infty du\,\tilde{\phi}_p(u)u^\omega\tilde{\psi}_q(u), \tag{43}$$

which exhibits a $|g|^{-\omega/(1+\omega)}$ scaling dependency. In Fig. 2 we have plotted the one-particle energy levels for $\omega = 1, 2, 3$,
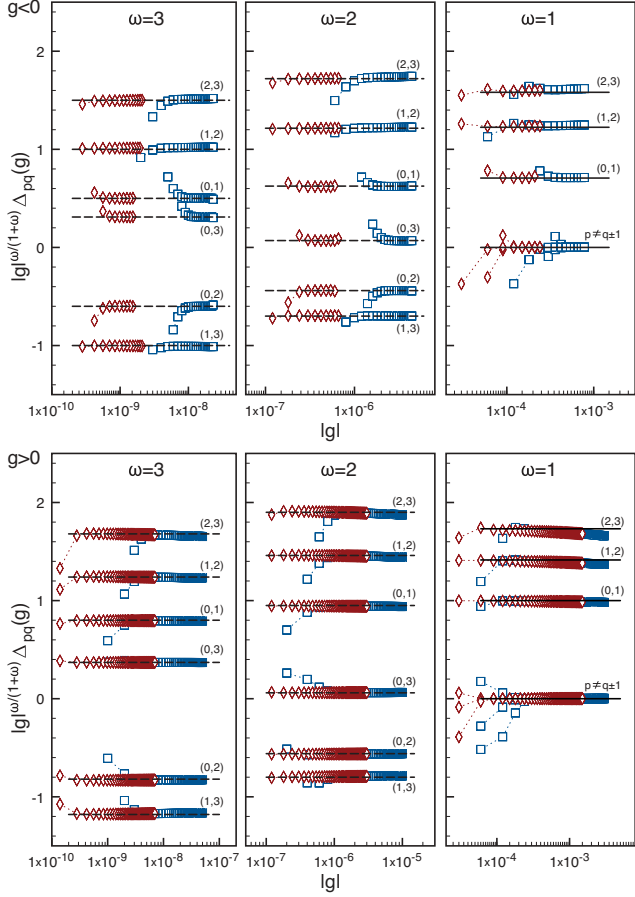
FIG. 3. (Color online) Scaling property in the ordered phase ($g < 0$) and in the disordered phase ($g > 0$) of the matrix elements (42) for different values of the exponent ω. Different colors are used for distinguishing different sizes (blue squares for $L = 256$, red diamonds for $L = 512$). Also in this case, the plateau region shows the range of validity of the scaling relation (43). For $\omega = 2, 3$ the dashed lines are guides for the eyes. For $\omega = 1$, the straight lines show the dependence on pq as in (53) and one can notice the vanishing amplitude for $p \neq q \pm 1$.

showing the agreement with the scaling form (39). In Fig. 3 we present the scaling properties of the matrix elements (42), as deduced from (43), for different values of the exponent ω. Again, the agreement with the expected scaling is very good for large system sizes and small g values.

During the quench, the departure from the adiabatic ground state can be deduced from the instantaneous occupation number $n_q(t) = \langle \varphi(t)|\eta_q^\dagger(g(t))\eta_q(g(t))|\varphi(t)\rangle$ of mode q. Inserting the lowest-order expansion $|\varphi(t)\rangle \simeq |0(t)\rangle + \sum_{p,q} a_{pq}(t_0, t)|pq(g(t))\rangle$, one has for the density of q excitations

$$n_q(t) \simeq 4 \sum_p |a_{pq}(t_0, t)|^2. \qquad (44)$$

The total defect density is given by summing up all the contributions coming from each q level:

$$n(t) = \sum_q n_q(t). \qquad (45)$$

To see this explicitly, let us recall that, at any time t, the Ising quantum chain is diagonalized in terms of noninteracting fermionic particles. The adiabatic ground state is the vacuum state with respect to these fermions [$\eta_q(g)|0(g)\rangle = 0 \, \forall \, q$]. Consequently, the number of fermions on the top of the instantaneous vacuum gives the number of defects. For example, if one quenches the Ising chain toward its deep ferromagnetic phase ($h_n \simeq 0 \, \forall \, n$), then the two ground states there are the ferromagnetic states in the x direction $|\ldots \uparrow\uparrow\uparrow\uparrow\uparrow\uparrow \ldots\rangle$ and $|\ldots \downarrow\downarrow\downarrow\downarrow\downarrow\downarrow \ldots\rangle$. The final state of the chain after the quench is a superposition of states like $|\ldots \uparrow\uparrow\uparrow\downarrow\downarrow\downarrow\uparrow\uparrow\uparrow\downarrow \ldots\rangle$ with finite domains separated by kinks. The number of such kinks is given by the operator $N = \frac{1}{2}\sum_n(1 - \sigma_n^x\sigma_{n+1}^x)$ and it is easy to show that it is given by $\sum_q \eta_q^\dagger\eta_q$ where the η are the corresponding creation and annihilation operators diagonalizing the chain at $h_n \simeq 0, \forall \, n$. This will remain true at all finite values of the transverse field, the only difference being that the number of defects is still given by $\sum_q \eta_q^\dagger(h)\eta_q(h)$ but no more by the kink number operator $N = \frac{1}{2}\sum_n(1 - \sigma_n^x\sigma_{n+1}^x)$, since, at $h \neq 0$, the basic excitations over the ground state are no longer kinks (even if they will be close to kinks as soon as we enter into the ferromagnetic regime).

The density of defects at a given lattice site can be deduced from the total defect density operator $\hat{n}(g) \equiv \sum_q \eta_q^\dagger(g)\eta_q(g) \equiv \sum_i \hat{n}_i(g)$, where the second sum runs over the space variable. Using the representations (37) of the Fermi operators, one obtains $\hat{n}(g) = \sum_i \frac{1}{2}\{1 - i\sum_{j,q} \phi_q(i,g)\psi_q(j,g)\Gamma_j^2\Gamma_i^1\}$, from which one can identify the local defect operator

$$\hat{n}_i(g) \equiv \frac{1}{2}\left\{1 - i\sum_{j,q} \phi_q(i,g)\psi_q(j,g)\Gamma_j^2\Gamma_i^1\right\}. \qquad (46)$$

The local density of defects generated at site i and at time t is then simply given by

$$n_i(t) \equiv n(i,t) \equiv \langle \varphi(t)|\hat{n}_i(g(t))|\varphi(t)\rangle. \qquad (47)$$

Another quantity much used in order to quantify the deviation from adiabaticity is the so called fidelity, $\mathcal{F}(t) \equiv |\langle 0(t)|\varphi(t)\rangle|^2$. In our approximation it is given by

$$\mathcal{F}(t) \simeq 1 - \sum_{p,q} |a_{pq}(t)|^2 = 1 - \frac{1}{4}\sum_q n_q(t), \qquad (48)$$

and then trivially deduced from the knowledge of the populations n_q. One can also consider the excess energy with respect to the instantaneous adiabatic ground state

$$e(t) = \langle \mathcal{H}(t)\rangle_t - E_0(g) = \sum_q \epsilon_q(g)n_q(t), \qquad (49)$$

which, in the first-order adiabatic approximation, becomes

$$e(t) = \langle \mathcal{H}(t)\rangle_t - E_0(g) \approx 4\sum_{p,q} \epsilon_p(g)|a_{pq}(t)|^2. \qquad (50)$$

B. Exact solution for the linear spatial perturbation

For a linear spatial modulation (i.e., at $\omega = 1$), the differential equations (40) can be explicitly solved in the thermodynamical limit $L \to \infty$ since the problem reduces to

a quantum one-dimensional harmonic oscillator. The Bogoliubov coefficients are given by the wave functions χ_p (up to normalization) of the harmonic oscillator [11]:

$$\phi_p(x) = |g|^{1/4}\sqrt{2}\chi_{2p}(u),$$
$$\psi_p(x) = \text{sgn}(g)|g|^{1/4}\sqrt{2}\chi_{2p+\text{sgn}(g)}(u), \quad (51)$$
$$\epsilon_p = |g|^{1/2}\sqrt{4p+1+\text{sgn}(g)}.$$

The functions χ_n are normalized in $[-\infty,\infty]$ so that $\sqrt{2}\chi_n$ are correctly normalized in $[0,\infty]$ and we have assumed $\chi_{-1}(u) \equiv 0$. The matrix elements $\langle pq(g)|\partial_g \mathcal{H}(g)|0(g)\rangle$ in (29) are then proportional to the position matrix elements of the harmonic oscillator $(\chi_p, u\chi_q)$, such that the only nonvanishing transition amplitudes $a_{pq}(t_0, t)$ are those with $p = q \pm 1$.

Plugging the exact solution into (29) one obtains a closed expression for the amplitudes a_{pq}. However, contrary to the spatial homogeneous case ($\omega = 0$) where the integral (29) converges at the critical value $g = 0$, here the linear spatial inhomogeneity modifies the dependence on g of the integrant to a g^{-1} behavior, leading to a logarithmic divergence at $g = 0$. This divergence is caused by the square root dependence on $|g|$ of the excitation spectrum $\epsilon_p = |g|^{1/2}\sqrt{4p+1+\text{sgn}(g)}$ with $p = 0, 1, 2, \ldots$ [11]. Consequently, the first-order adiabatic expansion (29) breaks down at the critical point $g = 0$ (i.e., at time $t = 0$). Nevertheless, for quenches that do not cross the critical point (the starting and the ending point of g are on the same side of the critical locus), one can still use (29) and one has explicitly

$$|a_{pq}(t_0, t)|^2 = \left|\frac{\Delta_{pq}}{2\Omega_{pq}}A_{\rho_{pq}}(|g_0|, |g(t)|)\right|^2, \quad (52)$$

with

$$\Delta_{pq}(g) = \sqrt{\frac{p+q}{2} + \frac{1+\text{sgn}(g)}{4}}[\delta_{p\,q-1} - \delta_{p\,q+1}], \quad (53)$$

$\Omega_{pq}(g) = |g|^{-1/2}\delta\omega_{pq,0}(g) = |g|^{-1/2}[\epsilon_p(g) + \epsilon_q(g)]$ and $\rho_{pq} = -2\Omega_{pq}\frac{v^{-1/\alpha}}{\alpha+2}\text{sgn}(g)$. The function

$$A_\rho(x, y) = \frac{2\alpha}{2+\alpha}\left[E_1\left(i\rho x^{\frac{2+\alpha}{2\alpha}}\right) - E_1\left(i\rho y^{\frac{2+\alpha}{2\alpha}}\right)\right] \quad (54)$$

is expressed in terms of the exponential integral $E_1(z) = \int_z^\infty dt\, t^{-1}e^{-t}$ for $|\text{Arg}(z)| < \pi$.

Let us discuss this analytical result. Consider first the case where the quench starts far away from the critical point, $|g_0| \gg 1$; that is, in an almost uncorrelated initial state. In that case, since $|g_0| \gg 1$ we have $E_1(i\rho|g_0|^{\frac{2+\alpha}{2\alpha}}) \simeq 0$ and the function $A(x, y)$ entering into (52) is dominated by the contribution of its second argument:

$$A_\rho(|g_0|, |g(t)|) \simeq -\frac{2\alpha}{2+\alpha}E_1\left(i\rho|g(t)|^{\frac{2+\alpha}{2\alpha}}\right). \quad (55)$$

Recalling that $\rho \propto v^{-1/\alpha}$ and $|g(t)| = v|t|^\alpha$, one recovers precisely the expected scaling behavior $n_q(g_0; t, v) = f(v|t|^{2+\alpha})$, with $y_v = 2 + \alpha$, which corresponds to the prediction (8) with $\nu = z = 1$ for the critical Ising chain and $\omega = 1$ for a spatial linear perturbation.

If the initial gradient g_0 is not sufficiently large, one can no longer neglect the contribution to $A_\rho(|g_0|, |g(t)|)$ of

its first argument. Consequently, after the quench one observes the nonhomogeneous behavior $n_q(g_0; t, v) \sim f_0(g_0) + f_1(|t|v^{1/y_v})$. The expected scaling behavior (8) is broken by the presence of the boundary term $f_0(g_0)$, which accounts for the high correlations in the initial ground state $|0(g_0)\rangle$ (since g_0 is not far from the critical point).

For a quench at or crossing the critical point, the situation is more complicated since, as stated before, the (un-normalized) perturbation formula (29) leads to a divergence at $t = 0$. However, for a finite-size chain, the energy gap $\delta\omega_{k0}$ stays finite at the critical points which wash out the critical divergences, and one can perform a finite-size scaling study.

C. Numerical analysis

1. Finite-size scaling analysis for general ω

For the general ω case, we have performed a numerical study with the following protocol: we start far away in the disordered phase with a fixed initial value $g = 1$ and drive the system to the critical point $g = 0$. The density of defects $n = \sum_q n_q$ and energy excess $e = \langle\mathcal{H}(t)\rangle_t - E_0(g)$ are calculated from (45) and (49), respectively. The numerical results are obtained by exact diagonalization of finite chains with up to 256 spins and the finite-size data are then extrapolated to the infinite-size limit. For a given set of ω and α values, we have done numerical diagonalization on systems with sizes from $L = 16$ to $L = 256$ sites, by steps of $\Delta L = 16$ obtaining 16 data sets. For each system size we have varied the amplitude v from a very small value ($v = 10^{-5}$) up to the relatively large value $v = 0.5$. In order to extract the asymptotic infinite-size behavior we have assumed, for any v, the finite-size scaling of the defect density

$$n(v, L) = n(v) + f_1(v)L^{-\lambda_c} + f_2(v)L^{-2\lambda_c} + \cdots, \quad (56)$$

where λ_c is an unknown correction to scaling exponent (the same procedure was used for the energy density). The second-order correction to scaling was kept in order to describe correctly the behavior at small v. The fit was done by looking for a global value of the scaling exponent λ_c independently on v. Defining the fitting function $F(v, x, \lambda) = A(v) + B(v)x^\lambda + C(v)x^{2\lambda}$, we have performed, for each value of v, a linear fit of the data varying the fit exponent λ in a reasonable range $[\lambda^{\min}, \lambda^{\max}]$. For a given v and λ we have then obtained the best parameters $\{A^*(v, \lambda), B^*(v, \lambda), C^*(v, \lambda)\}$. Looking for the minimum of the global least square function $\chi^2(\lambda) = \frac{1}{N-3}\sum_v\sum_x[n(v, x) - F^*(v, x, \lambda)]^2$, with $F^* = A^* + B^*x^\lambda + C^*x^{2\lambda}$, we have obtained the best global correction to the scaling exponent λ^* and identified the infinite-size value $n(v)$ with the coefficient $A^*(v, \lambda^*)$. We have also checked the stability of the fit under the variation of the number N of data sets used in the fitting procedure. The results are reported in Figs. 4 and 5 for the total defect density and for the energy excess, respectively, for different spatial and temporal exponents ω and α.

First of all, we observe that the finite-size values are always smaller than the extrapolated ones. Indeed, on the finite system the gap does not vanish even close to the critical locus and, consequently, the generation of defects is smaller than the expected one in the thermodynamical limit. At small v the
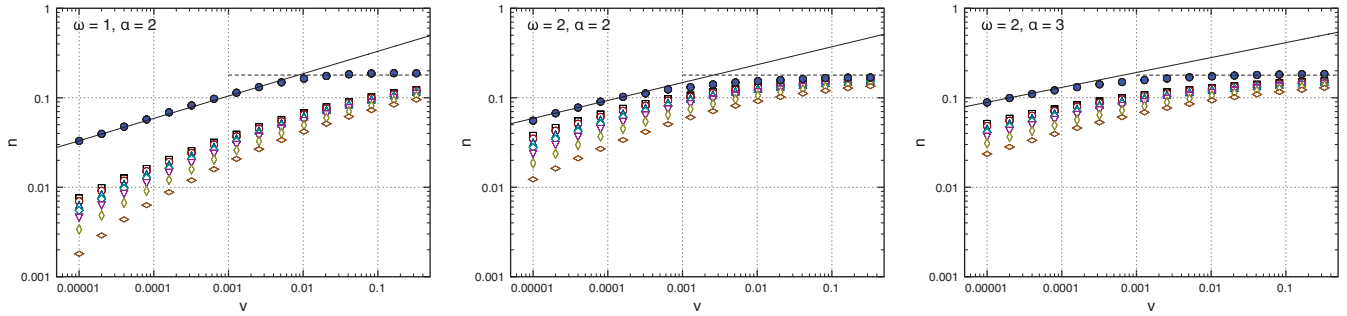
FIG. 4. (Color online) Density of defects n versus the quench parameter v for a critical quench. The amplitude changes from $g = 1$ to $g = 0$. Empty symbols correspond to different system sizes ($L = 96$ to $L = 256$ from bottom to top). The extrapolated data (filled circles) show, in the adiabatic limit, $v \ll 1$, a perfect agreement with the scaling prediction: $n \sim v^{1/4}$ for $\omega = 1, \alpha = 2$; $n \sim v^{1/5}$ for $\omega = 2, \alpha = 2$; and $n \sim v^{1/6}$ for $\omega = 2, \alpha = 3$ (straight lines). The dashed lines give the sudden-quench value $n_{sq} \approx 0.179$ evaluated on a system with $L = 1024$ spins.

extrapolated data are in perfect agreement with the scaling predictions $n \sim v^{d/y_v}$ and $e \sim v^{(d+z)/y_v}$ with $d = z = 1$, which are represented by the full lines. As the quench amplitude v is getting larger, we observe a crossover from the inhomogeneous Kibble-Zurek scaling scenario predictions toward a regime which is independent of the quench protocol (α and ω values) at large v. The observed saturation at large v of the defect production and of the energy excess is due to the fact that, for very fast quenches, the only relevant parameters are the initial and final amplitudes g. Indeed, if the initial amplitude is very high in modulus, the correlation length is very small (of the order of the lattice spacing) and the initial state is very close to the completely disordered state. Consequently, there is almost no difference for different values of ω. One expects the same defect production (and same energy excess) as in the case of a sudden quench of a completely disordered initial state toward the critical point. This is shown in Figs. 4 and 5 by the horizontal dashed lines which match perfectly the actual extrapolated numerical data. A similar behavior is reported in [25] where, for sufficiently fast inhomogeneous quenches, one recovers the homogeneous defect production (corresponding here to the homogeneous sudden-quench saturation at large v), while for sufficiently slow inhomogeneous quenches (here small v) the defect production is significantly lowered. The reason for this is that, when the inhomogeneity is switched off sufficiently fast, there is no causal connection between

different space points and the new phase starts to grow independently from every space point, which is exactly what happens in a homogeneous quench. On the contrary, if the unloading of the inhomogeneous perturbation is slow enough, the new phase nucleates from a single initial point (the critical locus) and communicates its phase through the whole system. Consequently, the defect production is lowered. Another way of understanding the crossover is by taking into account that, for a given v, the quench is done within a time $t_q = g^{1/\alpha} v^{-1/\alpha}$. The typical Kibble-Zurek time scale is given by $\tau_{KZ} = \tau_0 v^{-z/y_v}$. If the quench protocol time t_q is smaller than the Kibble-Zurek time τ_{KZ}, which happens at $v > v^*$ where v^* is deduced from $t_q|_v^* = \tau_{KZ}|_v^*$, then the dynamics start already from the very beginning in the sudden quench regime and there is no near-adiabatic evolution and one expects the same defect production as in a real sudden quench. On the other hand, for a larger value of t_q (i.e., a smaller value of v), the dynamics start first in a near-adiabatic regime, leading finally to a lower defect production.

2. Local density and global shift of the critical locus

In order to characterize the space dependence of the defects production, we have also computed the local defect density from the definition (46) and (47). The local density is expected to scale according to (13), where the appropriate scaling
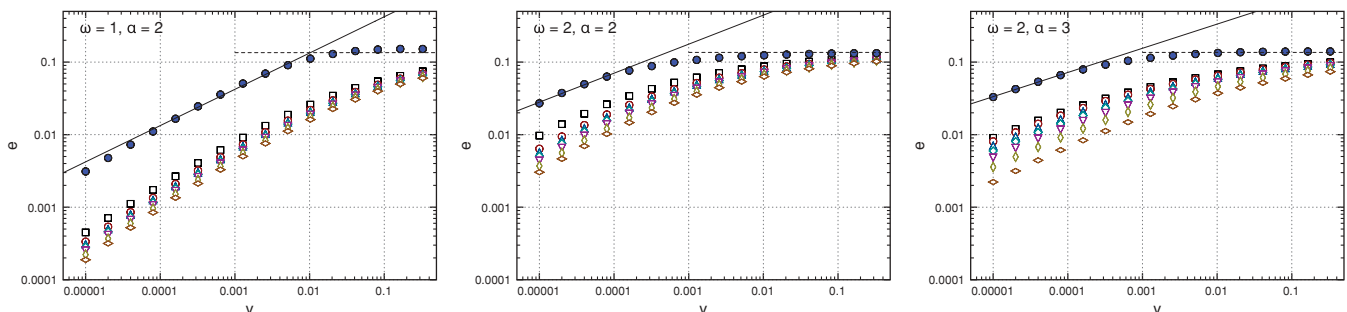

FIG. 5. (Color online) Energy density e versus the quench parameter v for a critical quench. The amplitude changes from $g = 1$ to $g = 0$. Empty symbols correspond to different system sizes ($L = 96$ to $L = 256$ from bottom to top). The extrapolated data (filled circles) show, in the adiabatic limit, $v \ll 1$, a perfect agreement with the scaling prediction: $n \sim v^{1/2}$ for $\omega = 1, \alpha = 2$; $n \sim v^{2/5}$ for $\omega = 2, \alpha = 2$; and $n \sim v^{1/3}$ for $\omega = 2, \alpha = 3$ (straight lines). The dashed lines give the sudden-quench value $e_{sq} \approx 0.136$ evaluated on a system with $L = 1024$ spins.
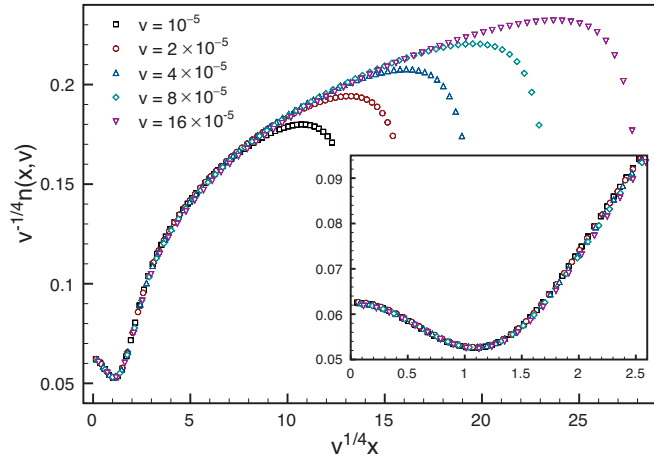
FIG. 6. (Color online) Rescaled local defect density as predicted by (13) for the Ising chain with $L = 256$, $\omega = 1$, and $\alpha = 2$. The quench is done from $g = 1$ to the critical point $g = 0$. The different lines correspond to different rates v. The scaling is expected to be valid for sufficiently small $v^{1/4}x$. The deviations on the right side at large arguments are finite-size effects. The inset shows the same as the main panel but zoomed close to the origin.

variable is $xv^{1/y_v} = x/\ell$. In Fig. 6 we have plotted the rescaled defect density $v^{-1/y_v}n(x,v)$ versus the scaling variable xv^{1/y_v} for a chain of size $L = 256$ and for a quench starting at $g = 1$ and ending at $g = 0$ with space exponent $\omega = 1$ (linear profile) and temporal ramp exponent $\alpha = 2$ for various values of v. The scaling is expected at small values of the scaling argument [which is shown in the inset of (6)] and, as seen in the figure, it is obviously satisfied. At large values of the scaling variable we observe a systematic finite-size deviation, which appears earlier for smaller values of v (larger values of the length scale $\ell = v^{1/y_v}$). We see clearly on this plot that the effect of the linear varying field is to reduce the defect production in the vicinity of the critical region, expelling out of it the generation of defects. Close to $xv^{1/y_v} = 0$, the nonmonotonic behavior is probably generated by the presence of the left boundary of the chain, which effectively lowers the local spin-spin couplings, facilitating then the generation of defects. The competition between this facilitation and the lowering of the defect production by the inhomogeneity close to the critical locus leads to the appearance of a locus of minimum defect generation which, from the inset of Fig. (6), is found around $xv^{1/y_v} = 1.1$.

When a small global shift δ_h is added to the system, one expects the modified scaling (23) for the defect density, which reduces to the linear shift (24) in the Ising-chain case, since $v = z = d = 1$. In Fig. 7, we have plotted the total density of defects in order to check the scaling prediction (24). The expected deviation to the zero-shift case is supposed to be linear but, nevertheless, we have represented the graph in a log-log scale in order to amplify the scaling region. One sees clearly on the figure that there is a perfect agreement between the numerical results and the scaling prediction over almost four decades.

At large negative shifts δ_h, the expected scenario developed in the preceding section is that of a complete fall down of the excitations in a causal region around the origin, where the

ordered phase propagates coherently through the disordered phase (without generating any defect), followed at large distances by a sudden increase of the defect production. This increase is due to the fact that the critical front propagates excessively fast through the disordered phase to permit a local relaxation of the phase to the new field parameters. We illustrate that in Fig. 8, where we have plotted the local density of defects for different shift values δ_h and rates v obtained numerically on a chain of size $L = 256$ with a linear perturbation ($\omega = 1$) and time-ramp exponent $\alpha = 2$. We observe that, for large values of $|\delta_h|$, there is indeed a drastic decay of the defect density that extends from the origin up to a threshold locus $x_0(\delta_h, v)$, after which the density
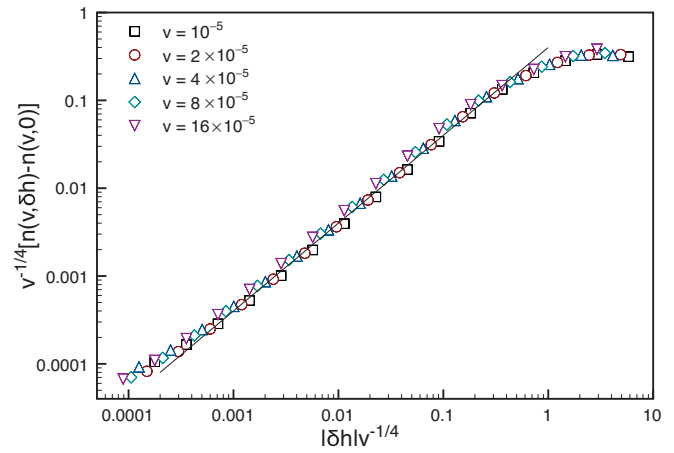

FIG. 7. (Color online) Rescaled defect density in the case of a finite global shift to the critical point as predicted by (24) for the Ising chain with $L = 256$, $\omega = 1$, and $\alpha = 2$. The quench is done from $g = 1$ to $g = 0$ at different rates v. The straight line represents the expected linear deviation to the $\delta_h = 0$ case.
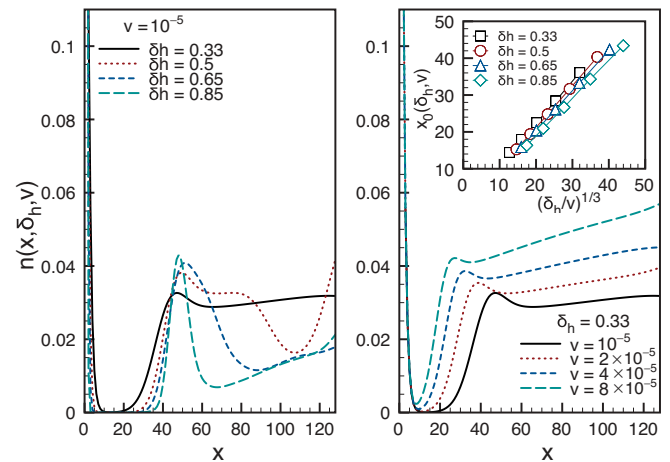

FIG. 8. (Color online) Local defect density in the case of a finite global shift to the critical point for the Ising chain with $L = 256$, $\omega = 1$, and $\alpha = 2$. The quench is done from $g = 1$ to $g = 0$. The left panel gives the behavior at fixed rate v for different values of the shift δ_h. The right panel shows the behavior at constant shift δ_h for different values of v. The inset gives the locus x_0 of the fast increase of the defect density as a function of the expected leading scaling behavior $(\delta_h/v)^{1/3}$.

suddenly increases. The pattern of the local density $n(x,\delta_h,v)$ at $x > x_0$ is much more complicated where secondary peaks appear and, consequently, it is hard to interpret this behavior. Nevertheless, the abrupt increase of the excitation density after a threshold locus validates the proposed scenario (see [22] where this scenario was developed for a critical front moving at constant velocity). In the inset of Fig. 8, we have drawn the dependence of the threshold locus x_0, extracted from the maximum of the spatial derivative of the density, versus the variable $(\delta_h/v)^{1/3}$, which corresponds for $\omega = 1$ and $\alpha = 2$ to the prediction (27) derived from the local scaling assumptions developed in Sec. II C. The agreement with (27), as seen from the inset of Fig. 8, is very good. One may have also extracted the $(\delta_h/v)^{1/3}$ behavior from the maximum of the first peak. However, doing so is a bit less convincing since broad secondary peaks have an influence on the position of the first maximum. Notice also that, very close to the origin, there is a density peak which falls off as $e^{-x/q(\delta_h)}$ on a v-independent length scale $q(\delta_h)$. Somehow a small finite density of excitations is trapped at the left boundary, while the remaining excitation density is rejected on the right of x_0.

V. DISCUSSION AND SUMMARY

In summary, we have developed a scaling theory which predicts the behavior of the nonlinear quench of a power-law perturbation close to a critical point. Such a power-law potential is relevant especially in the context of confined ultracold systems, where the dynamics are well described by the unitary evolution of closed systems. Within our scaling approach, we have derived the scaling properties of physical quantities like the density of defects or the energy excess generated during the loading or unloading of the power-law trap. The basic ingredient behind the scaling analysis is the identification of a so-called Kibble-Zurek time scale, which separates a nearly adiabatic regime from a sudden regime. This (Kibble-Zurek) time scale depends on the universal properties of the critical point as well as on the exponents characterizing the temporal ramp and the shape of the spatial trap. One of the main messages of this work is, in particular, that the optimal nonlinear way of crossing the critical point is strongly affected by the presence and the shape of the trapping potential. As a theoretical test of the scaling theory we have used the exactly solvable Ising model in a transverse field. The analysis revealed quite strong finite-size corrections, as seen in Fig. 4, to the expected scaling predictions for the density of defects and the energy excess. Nevertheless, the data extrapolated to the infinite-size limit fulfill very well the scaling predictions.

One of the main limitation of the present study with respect to a real experiment is that the dynamics driving the system are supposed to be unitary with no parasitic interactions at all with the environment, no extra dissipation, and no loss of quantum coherence. This, of course, is a serious limitation if one considers long protocol times. A relevant extension of the present work would be to take into account such extra interactions. The influence of temperature on the scaling predictions, as, for example, in [26], is also one of the more relevant extensions of this work that has to be done.

APPENDIX A: ADIABATIC PERTURBATIVE EXPANSION

We sketch briefly the demonstration of the nearly adiabatic approach used in this study. First, we discretize the time t so that we have $t_0, t_1, \ldots, t_n, \ldots, t_N = t$ with $dt = t_n - t_{n-1}$; ultimately we will take the limit $N \to \infty$, $dt \to 0$ with t fixed. The unitary time evolution operator is written as an expansion product

$$\mathcal{U}(t,t_0) = \mathcal{U}(t_N,t_{N-1}) \cdots \mathcal{U}(t_2,t_1)\mathcal{U}(t_1,t_0), \quad \text{(A1)}$$

where, in the limit $dt \to 0$, we have essentially

$$\mathcal{U}(t_{n+1},t_n) = e^{-i\mathcal{H}(t_n)\,dt}. \quad \text{(A2)}$$

Now, let us find an expression for the state after each small time interval.

a. $t_0 \to t_1$

The evolution starts from the initial ground state $|\varphi(t_0)\rangle = |0(t_0)\rangle$ at time t_0. The state at time t_1 is generated by the action of $\mathcal{U}(t_1,t_0) = e^{-i\mathcal{H}(t_0)\,dt}$, which leads to the appearance of a phase factor:

$$|\varphi(t_1)\rangle = e^{-iE_0(t_0)\,dt}|0(t_0)\rangle. \quad \text{(A3)}$$

b. $t_1 \to t_2$

At the next step we have

$$|\varphi(t_2)\rangle = \mathcal{U}(t_2,t_1)|\varphi(t_1)\rangle = e^{-i\mathcal{H}(t_1)\,dt}|\varphi(t_1)\rangle. \quad \text{(A4)}$$

Writing

$$\mathcal{H}(t_0) = \mathcal{H}(t_1) - \frac{\mathcal{H}(t_1) - \mathcal{H}(t_0)}{dt}dt \equiv \mathcal{H}(t_1) - \mathcal{W}(t_1,t_0)\,dt, \quad \text{(A5)}$$

we can expand the eigenvectors of $\mathcal{H}(t_0)$ in the basis of the eigenvectors of $\mathcal{H}(t_1)$ to first order in the perturbation $\mathcal{W}(t_1,t_0)\,dt$:

$$|0(t_0)\rangle = |0(t_1)\rangle + dt \sum_{n\neq 0} \frac{\langle n(t_1)|\mathcal{W}(t_1,t_0)|0(t_1)\rangle}{E_n(t_1) - E_0(t_1)}|n(t_1)\rangle, \quad \text{(A6)}$$

leading to

$$|\varphi(t_2)\rangle = e^{-i[E_0(t_0)+E_0(t_1)]dt}|0(t_1)\rangle + \sum_{n\neq 0}|n(t_1)\rangle dt\, e^{-iE_n(t_1)dt}$$
$$\times \frac{\langle n(t_1)|\mathcal{W}(t_1,t_0)|0(t_1)\rangle}{E_n(t_1) - E_0(t_1)}e^{-iE_0(t_0)dt}. \quad \text{(A7)}$$

Continuing along these lines, it is straightforward to prove by induction that, at t_k, we have

$$|\varphi(t_k)\rangle = e^{-i\sum_{j=0}^{k-1} dt E_0(t_j)}|0(t_k)\rangle$$
$$+ \sum_{n\neq 0}|n(t_k)\rangle \sum_{i=1}^{k} dt\, e^{-i\sum_{j=i}^{k-1} dt E_n(t_j)}$$
$$\times \frac{\langle n(t_i)|\mathcal{W}(t_i,t_{i-1})|0(t_i)\rangle}{E_n(t_i)-E_0(t_i)}e^{-i\sum_{j=0}^{i-1} dt E_0(t_j)}. \quad \text{(A8)}$$

Taking the limit $dt \to 0$ we have $\mathcal{W}(t_{n+1},t_n) \to \partial_t\mathcal{H}(t)|_{t_n}$, and one obtains finally

$$|\varphi(t)\rangle = e^{-i\int_{t_0}^{t} ds E_0(s)}|0(t)\rangle + \sum_{n\neq 0}|n(t)\rangle \int_{t_0}^{t} dt'\, e^{-i\int_{t'}^{t} ds E_n(s)}$$
$$\times \frac{\langle n(t')|\partial_{t'}\mathcal{H}(t')|0(t')\rangle}{E_n(t')-E_0(t')}e^{-i\int_{t_0}^{t'} ds E_0(s)}. \quad \text{(A9)}$$

APPENDIX B: DYNAMICS IN THE ISING QUANTUM CHAIN

The initial state we start with is the ground state of $\mathcal{H}(g_0)$ associated to a given value $g_0 = g(t_0)$, and it is fully specified by the Clifford correlation matrix

$$\langle \mathbf{\Gamma}\mathbf{\Gamma}^{\dagger}\rangle_{t_0} = \begin{pmatrix} \langle \Gamma_m^1 \Gamma_n^1\rangle_{t_0} & \langle \Gamma_m^1 \Gamma_n^2\rangle_{t_0} \\ \langle \Gamma_m^2 \Gamma_n^1\rangle_{t_0} & \langle \Gamma_m^2 \Gamma_n^2\rangle_{t_0} \end{pmatrix} = \mathbb{I} + i \begin{pmatrix} \emptyset & \mathbf{G} \\ -\mathbf{G}^{\dagger} & \emptyset \end{pmatrix}, \quad \text{(B1)}$$

where

$$G_{mn} = \sum_k \phi_k(m,g_0)\psi_k(n,g_0). \quad \text{(B2)}$$

Splitting the continuum time evolution into N infinitesimal sudden quenches, the expectation of the Clifford correlation matrix at time t is given by

$$\langle \mathbf{\Gamma}\mathbf{\Gamma}^{\dagger}\rangle_{t} = \prod_{i=N}^{0} \mathcal{R}^T(dt;t_i)\langle \mathbf{\Gamma}\mathbf{\Gamma}^{\dagger}\rangle_{t_0} \prod_{i=0}^{N} \mathcal{R}(dt;t_i), \quad \text{(B3)}$$

where the infinitesimal evolution matrix for the time interval $[t_i,t_{i+1}]$ is

$$\mathcal{R}(dt;t_i) = \begin{pmatrix} \langle \Gamma_m^1|\Gamma_n^1\rangle_{t_i} & \langle \Gamma_m^1|\Gamma_n^2\rangle_{t_i} \\ \langle \Gamma_m^2|\Gamma_n^1\rangle_{t_i} & \langle \Gamma_m^2|\Gamma_n^2\rangle_{t_i} \end{pmatrix}, \quad \text{(B4)}$$

with the time-dependent contractions

$$\langle \Gamma_m^1|\Gamma_n^1\rangle_{t_i} = \sum_k \phi_k(m,t_i)\phi_k(n,t_i)\cos[\epsilon_k(t_i)\,dt],$$
$$\langle \Gamma_m^1|\Gamma_n^2\rangle_{t_i} = -\sum_k \phi_k(m,t_i)\psi_k(n,t_i)\sin[\epsilon_k(t_i)\,dt],$$
$$\langle \Gamma_m^2|\Gamma_n^1\rangle_{t_i} = \sum_k \psi_k(m,t_i)\phi_k(n,t_i)\sin[\epsilon_k(t_i)\,dt],$$
$$\langle \Gamma_m^2|\Gamma_n^2\rangle_{t_i} = \sum_k \psi_k(m,t_i)\psi_k(n,t_i)\cos[\epsilon_k(t_i)\,dt]. \quad \text{(B5)}$$

Taking the limit $N \to \infty$, $dt = t_i - t_{i-1} \to 0$, we recover the continuous time evolution.

Using the time evolution (B3) and the mapping between Clifford's operators and free-fermion operators we can easily write the evolution of the free-fermion correlation matrix

$$\begin{pmatrix} \eta \\ \eta^{\dagger T} \end{pmatrix} \cdot (\eta^{\dagger} \; \eta^T)$$

as

$$\begin{pmatrix} \langle \eta\eta^{\dagger}\rangle & \langle \eta\eta^T\rangle \\ \langle \eta^{\dagger T}\eta^{\dagger}\rangle & \langle \eta^{\dagger T}\eta^T\rangle \end{pmatrix}(t) = \frac{1}{4}\mathbf{V}^{\dagger}(g)\langle \mathbf{\Gamma}\mathbf{\Gamma}^{\dagger}\rangle_t \mathbf{V}(g), \quad \text{(B6)}$$

where $\mathbf{V}(g)$ is the matrix [almost unitary since $\mathbf{V}(g)^{\dagger}\mathbf{V}(g) = 2\mathbb{I}$] relating Clifford operators to Fermi operators:

$$\begin{pmatrix} \mathbf{\Gamma}^1 \\ \mathbf{\Gamma}^2 \end{pmatrix} = \mathbf{V}(g) \begin{pmatrix} \eta(g) \\ \eta^{\dagger T}(g) \end{pmatrix}. \quad \text{(B7)}$$

Notice that the time dependence in (B6) is due to the temporal evolution of the Clifford correlation matrix and to the parametric dependence on time, through $g(t)$, of the free-fermion operators.

[1] S. Sachdev, *Quantum Phase Transitions* (Cambridge University Press, Cambridge, 1999).

[2] B. Berche and C. Chatelain, *Order, Disorder and Criticality*, edited by Yu. Holovatch (World-Scientific, Singapore, 2004), p 147; U. Grimm and M. Baake, *The Mathematics of Long-Range Aperiodic Order*, edited by R. V. Moody (Kluwer, Dordrecht, 1997); F. Igloi, D. Karevski, and H. Rieger, Eur. Phys. J. B **1**, 513 (1998); **5**, 613 (1998); D. Karevski *et al.*, *ibid.* **20**, 267 (2001).

[3] F. Iglói, I. Peschel, and L. Turban, Adv. Phys. **42**, 683 (1993).

[4] K. Binder, *Phase Transitions and Critical Phenomena*, edited by C. Domb and J. L. Lebowitz (Academic Press, London, 1983), Vol. 8, p. 1.

[5] J. L. Cardy, J. Phys. A: Math. Gen. **16**, 3617 (1983); M. N. Barber, I. Peschel, and P. A. Pearce, J. Stat. Phys. **37**, 497 (1984); J. L. Cardy, Nucl. Phys. B **240**, 514 (1984); I. Peschel, Phys. Lett. A **110**, 313 (1985); D. B. Abraham and F. T. Latrémolière, J. Stat. Phys. **81**, 539 (1995); D. Karevski, P. Lajkó, and L. Turban, *ibid.* **86**, 1153 (1997); B. Davies and I. Peschel, Ann. Phys. Lpz. **6**, 187 (1997); I. Peschel, L. Turban, and F. Iglói, J. Phys. A: Math. Gen. **24**, L1229 (1991).

[6] H. J. Hilhorst and J. M. J. van Leeuwen, Phys. Rev. Lett. **47**, 1188 (1981); D. Karevski, G. Palagyi, and L. Turban, J. Phys. A: Math. Gen. **28**, 45 (1995).

[7] B. Sapoval, M. Rosso, and J. F. Gouyet, J. Phys. Lett. **46**, L149 (1985); M. Rosso, J. F. Gouyet, and B. Sapoval, Phys. Rev. B **32**, 6053 (1985); Phys. Rev. Lett. **57**, 3195 (1986); R. M. Ziff and B. Sapoval, J. Phys. A: Math. Gen. **19**, L1169 (1986); J. F. Gouyet, M. Rosso, and B. Sapoval, Phys. Rev. B **37**, 1832 (1988).

[8] T. Platini, D. Karevski and L. Turban, J. Phys. A **40**, 1467 (2007).

[9] W. H. Zurek and U. Dorner, Phil. Trans. R. Soc. A **366**, 2953 (2008).

[10] B. Damski and W. H. Zurek, New J. Phys. **11**, 063014 (2009); M. Campostrini and E. Vicari, Phys. Rev. Lett. **102**, 240601 (2009); e-print arXiv:0906.2640.

[11] M. Collura, D. Karevski and L. Turban, J. Stat. Mech. (**2009**) P08007.

[12] M. Greiner *et al.*, Nature (London) **415**, 39 (2002); M. Lewenstein *et al.*, Adv. Phys. **56**, 243 (2007); T. Kinoshita *et al.*, Nature (London) **440**, 990 (2006); L. E. Sadler *et al.*, *ibid.* **443**, 312 (2006).

[13] W. H. Zurek, U. Dorner, and P. Zoller, Phys. Rev. Lett. **95**, 105701 (2005).

[14] B. Damski, Phys. Rev. Lett. **95**, 035701 (2005); B. Damski and W. H. Zurek, Phys. Rev. A **73**, 063405 (2006); Phys. Rev. Lett. **99**, 130402 (2007); F. M. Cucchietti, B. Damski, J. Dziarmaga, and W. H. Zurek, Phys. Rev. A **75**, 023603 (2007).

[15] J. Dziarmaga, Phys. Rev. Lett. **95**, 245701 (2005); R. W. Cherng and L. S. Levitov, Phys. Rev. A **73**, 043614 (2006).

[16] A. Polkovnikov, Phys. Rev. B **72**, 161201 (2005); Phys. Rev. Lett. **99**, 130402 (2007); C. De Grandi, R. A. Barankov, and A. Polkovnikov, *ibid.* **101**, 230402 (2008); D. Sen, K. Sengupta, and S. Mondal, *ibid.* **101**, 016806 (2008); A. Polkovnikov and V. Gritsev, Nature Phys. **4**, 477 (2008).

[17] R. Barankov and A. Polkovnikov, Phys. Rev. Lett. **101**, 076801 (2008).

[18] T. W. B. Kibble, J. Phys. A **9**, 1387 (1976); Phys. Rep. **67**, 183 (1980); W. H. Zurek, Nature (London) **317**, 505 (1985); Acta Physica Polonica B **24**, 1301 (1993).

[19] E. Farhi *et al.*, Science **292**, 472 (2001).

[20] M. Collura and D. Karevski, Phys. Rev. Lett. **104**, 200601 (2010).

[21] J. A. Hertz, Phys. Rev. B **14**, 1165 (1976).

[22] J. Dziarmaga and M. M. Rams, New J. Phys. **12**, 055007 (2010); **12**, 103002 (2010); J. Dziarmaga, Adv. Phys. 1 (2010).

[23] F. Iglói and H. Rieger, Phys. Rev. Lett. **85**, 3233 (2000); D. Karevski, Eur. Phys. J. B **27**, 147 (2002); G. M. Schütz and S. Trimper, Europhys. Lett. **47**, 164 (1999); S. Dorosz, T. Platini, and D. Karevski, Phys. Rev. E **77**, 051120 (2008); T. Platini and D. Karevski, J. Phys. A: Math. Theor. **40**, 1711 (2007); V. Eisler, D. Karevski, T. Platini and I. Peschel, J. Stat. Mech. (**2008**) P01023.

[24] The scaling prescription $gL^\omega = $ const. insures that we are describing the system in the vicinity of the critical region only.

[25] T. W. B. Kibble and G. E. Volovik, JETP Lett. **65**, 102 (1997); J. Dziarmaga, P. Laguna, and W. H. Zurek, Phys. Rev. Lett. **82**, 4749 (1999); W. H. Zurek, *ibid.* **102**, 105702 (2009).

[26] D. Patanè, A. Silva, L. Amico, R. Fazio, and G. E. Santoro, Phys. Rev. Lett. **101**, 175701 (2008); D. Patanè, L. Amico, A. Silva, R. Fazio, and G. E. Santoro, Phys. Rev. B **80**, 024302 (2009).